Possibility for transoceanic tsunami forecast by numerical simulation—Example of 1960 Chilean tsunami by numerical simulation

Kazuaki Takaoka[1], Kazuhiko Ban[1], and Shigeru Yamaki[2]

[1]***Electric Power Development Company, Tokyo, Japan***
[2]***Seamus Limited, Toyosaka, Niigata-ken, Japan***

Abstract. In this study, using a fault model, the authors performed the numerical simulation of the tsunami propagated across the Pacific Ocean in connection with the 1960 Chile Earthquake, and obtained a good match in the comparison of the calculation results and the records of observed inundation heights and tide gauges distributed along the Japanese coast. In this simulation, it was confirmed that the short-period components decayed by diffusion and the transoceanic tsunami waves consequently became long-period dominant, in addition to the tsunami source with a long-period component itself. Furthermore, it was found that estimation errors of fault parameters have little influence on tsunami wave heights calculated for the Japanese coast. As the time required for calculations is approximately 11 hours, it is possible enough to carry out real-time numerical forecasts before a transoceanic tsunami arrival.

1. Introduction

The 1960 Chilean tsunami, which occurred with the Chile earthquake on 24 May 1960, struck the Japanese coast with severe damage 22 hours after the earthquake occurred. Imamura *et al.* (1990), Goto and Sato (1993), and Tanioka (2000), among others, have studied a transoceanic tsunami and established the basic method for the tsunami performance forecast using the numerical simulation. Nowadays, since computer capacity has made rapid progress, it has become possible to use computers for numerical forecasts, shortening the calculation time and improving calculation accuracy. This study shows the possibilities of forecast for the periodic characteristics of transoceanic tsunamis, the effects of parametric errors in tsunami sources, and actual calculating times in the case of the 1960 Chilean tsunami.

2. Simulation Method

The numerical simulations were composed of two stages: the calculations for the entire Pacific region (hereinafter "trans-Pacific propagation calculation") and for the Japanese coastal region (hereinafter "Japanese coastal calculation").

In the trans-Pacific propagation calculation, the linear Boussinesq equation in the polar coordinate system is used, considering the wave diffusion in long distant propagation and the influence of Coriolis force. This is similar to the method of Imamura *et al.* (1990) and Goto and Sato (1993). The

[1]Electric Power Development Co., Nuclear Power Dept., 6-15-1, Ginza, Chuou-ku, Tokyo, 104-8165, Japan (kazuaki_takaoka@epdc.co.jp)
[2]Seamus Ltd., 2235 Kizaki, Toyosaka-City, Niigata-Pre., Japan (yamaki@kc4.so-net.ne.jp)

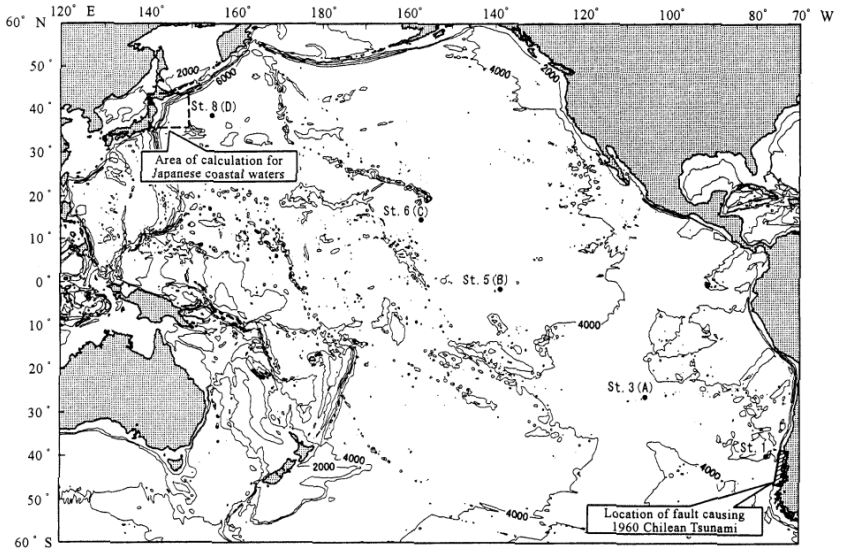

Figure 1: Area of calculations for trans-Pacific propagation.

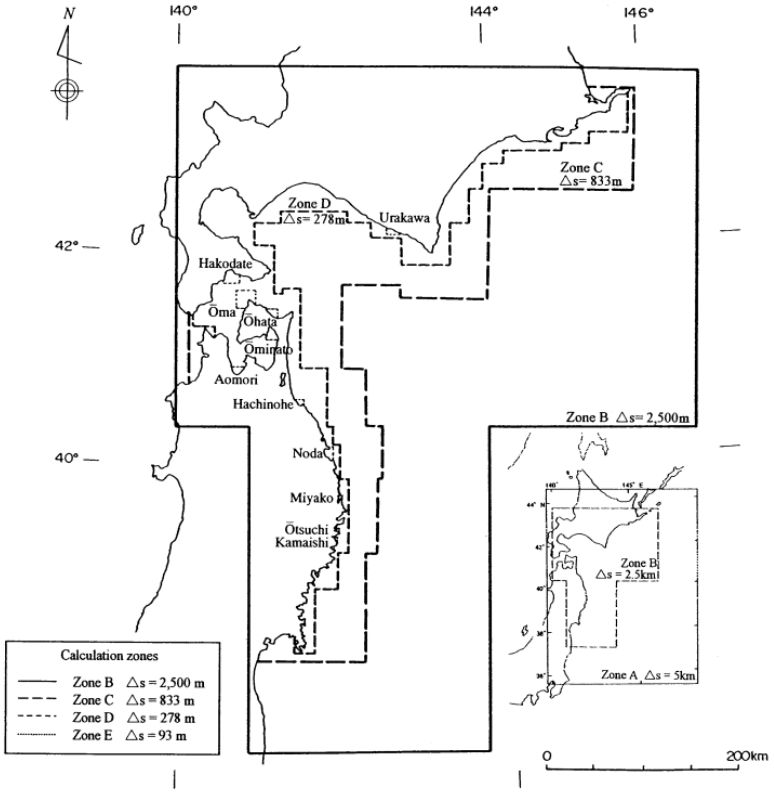

Figure 2: Area of Japanese coastal calculations.

Table 1: Fault parameters of tsunami source model taken.

		Parameter	Remark
Fault length	L	800 km	According to Kanamori and Cipar (1974)
Fault width	W	200 km	”
Slip	D	24 m	”
Inclination	δ	10°	”
Slip angle	λ	90°	”
Strike	θ	N10°E	”
Top depth of fault plane	d	1 km	Set up due to proximity to trench axis

calculation area is shown in Fig. 1. The calculation grid size is 10 min in both longitude and latitude, which is approximately equal to 18.5 km at the equator. The initial conditions are given from the sea floor displacement, calculated by a fault model using the method of Mansinha and Smylie (1971). The time step of calculations is 20 seconds.

In Japanese coastal calculations, the shallow water theory, which applies a non-linear long-wave equation, is used in the same method as Goto and Sato (1993). The rectangular coordinate system was used for the calculation shown in Fig. 2. The grid size consists of subdividing 5 × 5 km grids (Zone A) in offshore, 278 × 285 m grids (= 2.5 km/9; Zone D) and 93 × 93 m grids (= 2.5 km/27; Zone E) for the whole of the main calculating shore. Furthermore, the tsunami run-up to land area was also calculated at 93 × 93 m grids, based on the condition of Iwasaki and Mano (1979). The time step of the calculations is 1 second.

3. Reproducibility of 1960 Chilean Tsunami by Simulation

Table 1 shows fault parameters based on the model of Kanamori and Cipar (1974). Figures 3a and b indicate, respectively, the fault location and the distribution of the initial vertical displacement on the sea floor. As for the fault, the authors moved the fault location, which was described by Imamura *et al.* (1990), eastward to correspond to the trench axis. The top depth of the fault plane was supposed to be at 1 km, because the earthquake hypocenter was close to the trench axis, which suggested the hypocenter was extremely shallow.

As a result of the calculation, Fig. 4 shows the distribution of observed inundation heights and calculated wave heights along the Japanese coast. In order to verify if the calculation result is adequate, the indices of K and κ, which were proposed by Aida (1978), were also calculated in 117 points of 93 × 93 m grids (Zone E). A geometrical average of K = 1.06 and logarithmic standard deviation of κ = 1.40 indicate good reproducibility. In the case of extending the calculation area to 278 × 278 m grids (Zone D) including 290 points, those indices became K = 1.04 and κ = 1.55, and the reproduced tsunami wave height slightly scatters accordingly.

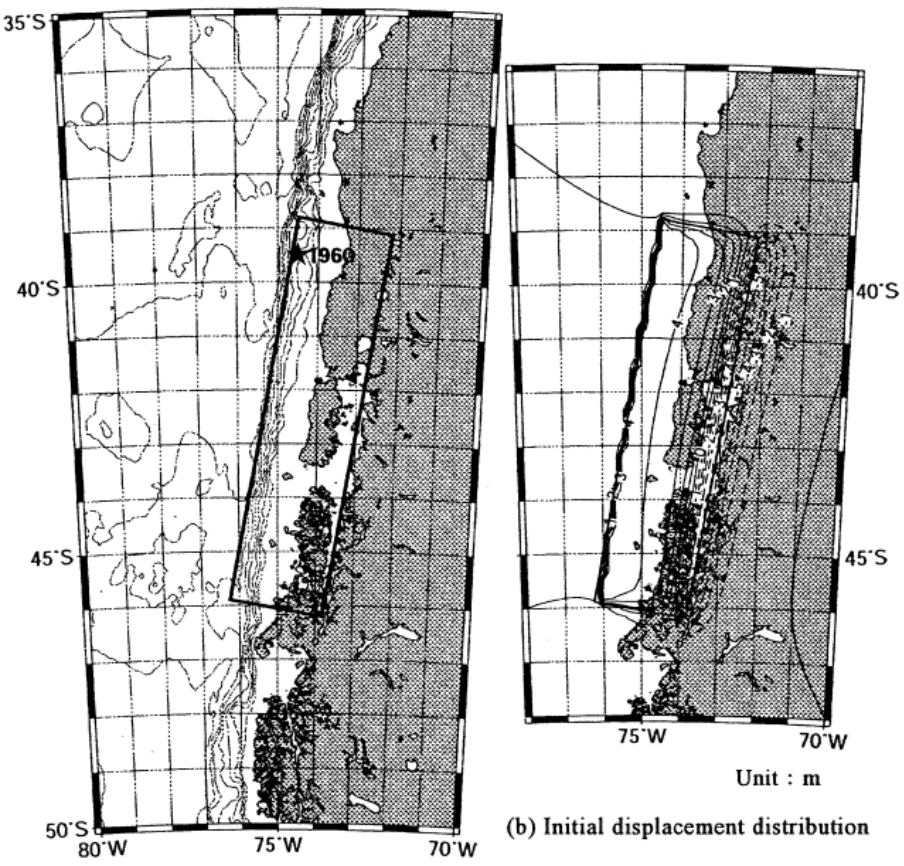

Figure 3: Tsunami fault model.

Furthermore, Fig. 5 shows the wave characteristics observed by tide gauges, compared with the calculated ones, in the representative four cities, Hakodate, Aomori, Oominato, and Hachinohe. It was confirmed that the calculations in four tide-gauge points indicate good reproducibility in wave heights and periods.

4. Considerations Concerning Forecast Accuracies and Calculation Time

4.1 Periodic characteristics of transoceanic tsunamis

As mentioned above, it was confirmed that the tide record could be reproduced well by an adequate method. It was supposed that the good reproducibility in the calculated wave was also due to the record obtained easily by tide gauges, because the transoceanic tsunami was generally predominant in the long-period component. The following discussions deal with the predominant period of calculated waves and the decay of short-period components by sea mounts.

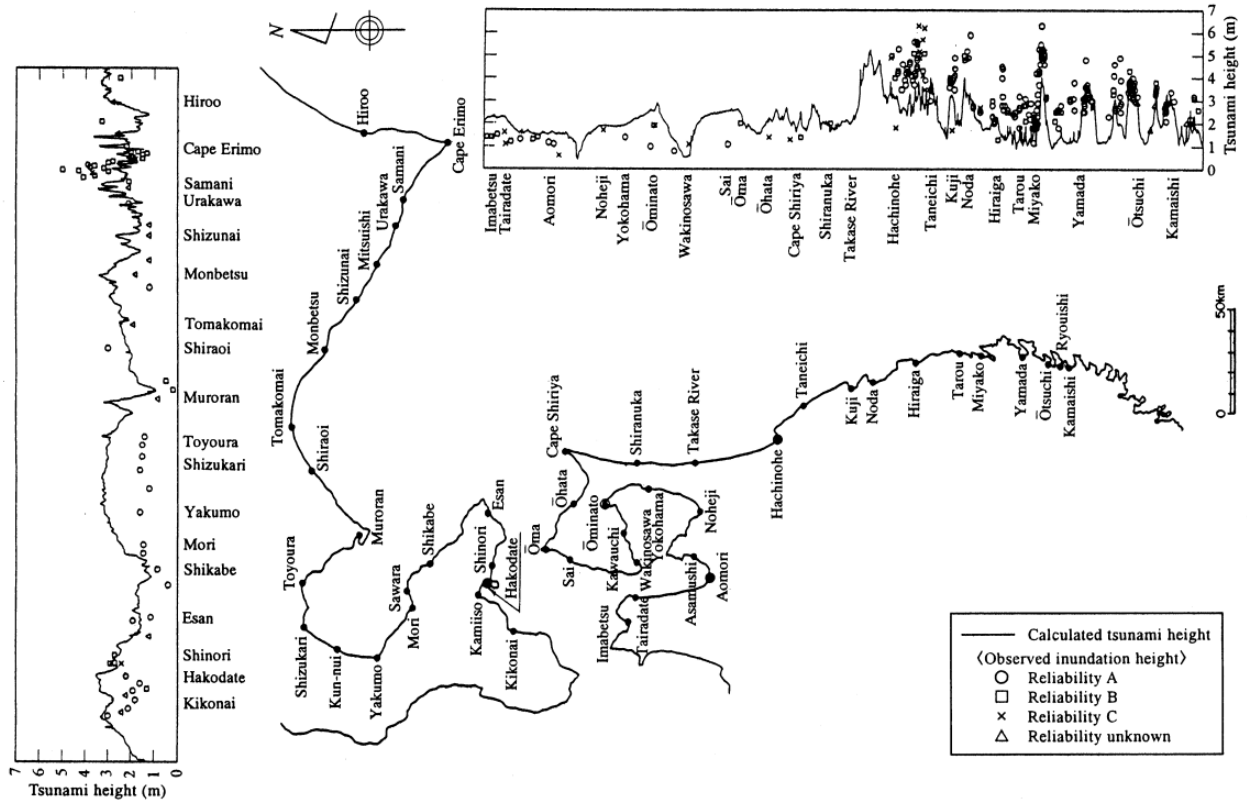

Figure 4: Distribution of tsunami heights in Japanese coast.

4.1.1 Periodic characteristics of calculated waves

Figure 6 shows the water level changes at representative points in the trans-Pacific propagation calculation. At the St. 1 point close to the earthquake hypocenter, the period of the initial wave indicates the long period of approximately 150 min. At the St. 5 point on the intermediate point of trans-Pacific and the St. 8 point near the coast of Japan, both first waves also indicate the long period of 120 to 150 min. This suggests that the 1960 Chilean tsunami was predominant in long-period component.

4.1.2 Diffusion and decay due to sea mounts

Tsuji (1991) says that in case there is a sea mount (height: H, diameter of foot contour: D) with a height of two-dimensional normal distribution shape in the uniform depth (h_0), the energy ratio between the diffused wave and the source tsunami, which is a normal distribution shaped tsunami (wavelength considered as $L = 4\sigma$), could be evaluated as a diffusion width (ℓ).

Based on the method of Tsuji (1991), the authors calculated the diffusion and the decay energy ratio in the trans-Pacific propagation of the 1960 Chilean tsunami. Figure 7 shows the result in each period, and indicates

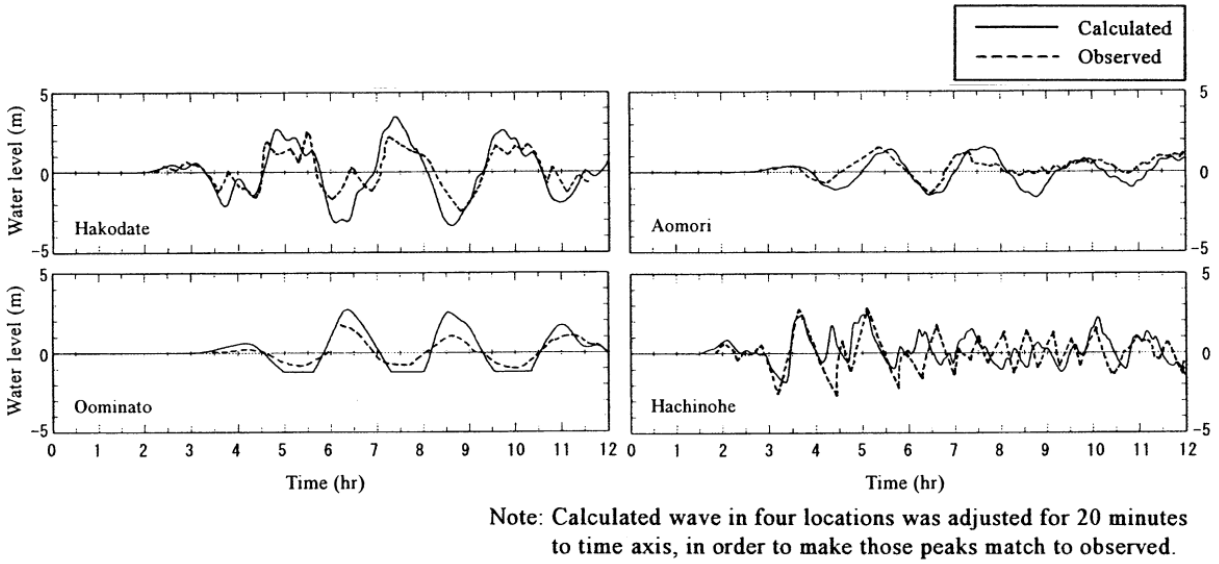

Figure 5: Observed and calculated waves at various locations along Japanese coast.

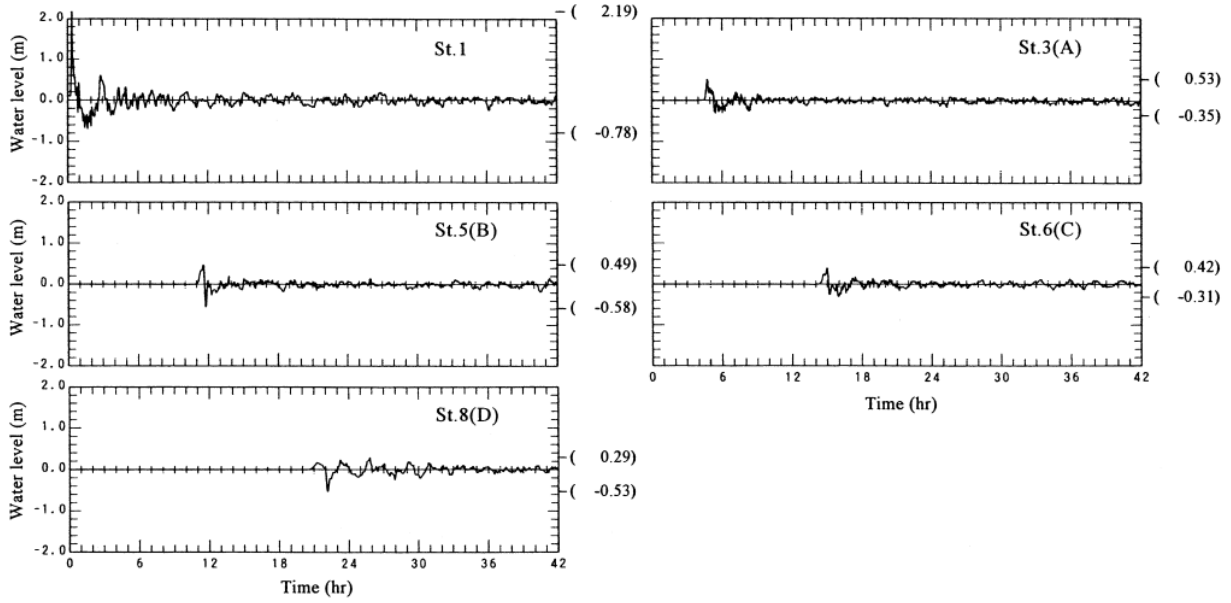

Figure 6: Water level changes at the representative points in trans-Pacific propagation calculations.

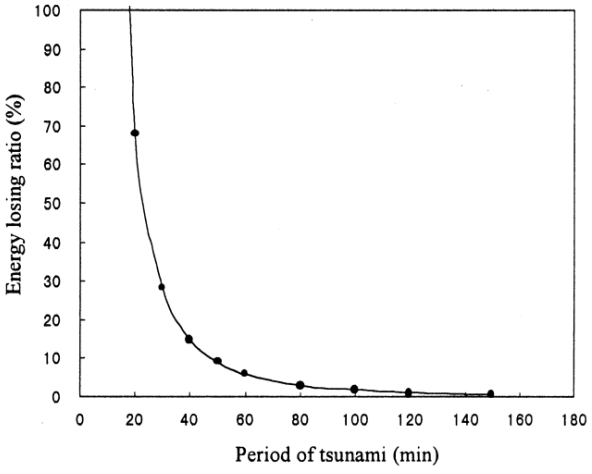

[equations]

$$R = \sum \frac{l}{b} \times 100(\%)$$

$$\because l = \frac{E_s}{E_I} = \frac{\pi^{3/2} H^2 \sigma r_0^{\,4}}{4h_0^{\,2}\left(4r_0^{\,2}+\sigma^2\right)^2} \cdot \frac{\left(\alpha^4+2\alpha^3-2\alpha^2+2\alpha+1\right)}{\alpha^3(\alpha+1)^2}$$

$$r_0 \fallingdotseq \frac{D}{4}, \quad \alpha = \sqrt{\frac{\sigma^2}{4r_0^{\,2}+\sigma^2}}, \quad \sigma = \frac{L}{4}$$

R : loss ratio
b : width of diffusion
l : diffusion width (length in y direction corresponding to energy lost due to diffusion)
E_s : total quantity of total energy of diffused waves
E_I : total energy per unit length in y direction of incident tsunami

Figure 7: Energy losing ratio due to diffusion in propagation from Chilean offshore to Japanese coast.

that the decay begins to occur at approximately 50 min and that the decay ratio of the period shorter than 20 min becomes very high.

As mentioned above, it is thought that the calculation produced good matches with the observed records because the long-period component predominantly reaches the Japanese coast in transoceanic tsunamis, and the tide-gage records with sufficient accuracy were obtained by the existing observation system.

4.2 Influence of estimation error in fault parameters on calculated tsunami wave height

The authors performed the parametric study of the influence that the error of the fault model parameter gives to the calculated tsunami wave height. The model of wave source used is the one based upon Kanamori and Cipar (1974) (hereinafter "K&C model"). Furthermore, one case on the uniform slip distribution model, which was developed through the analysis of the earth crust movement by Barrientos and Ward (1990) (hereinafter "B&W model"), was calculated for comparison.

Table 2 shows the whole fault parameters of a tsunami source and the indices of K and κ, which suggests the average relation between the calculated tsunami wave heights and the observed inundation heights along the Japanese coast. The table also shows the inverse number of K (hereinafter "1/K") that indicates the average ratio of observed inundation heights and calculated tsunami wave heights. The 1/K suggests that the higher number means the larger calculated tsunami wave heights. Figure 8 shows these results in every parameter. The initial wave change in the main vertical profiles is shown in Fig. 9.

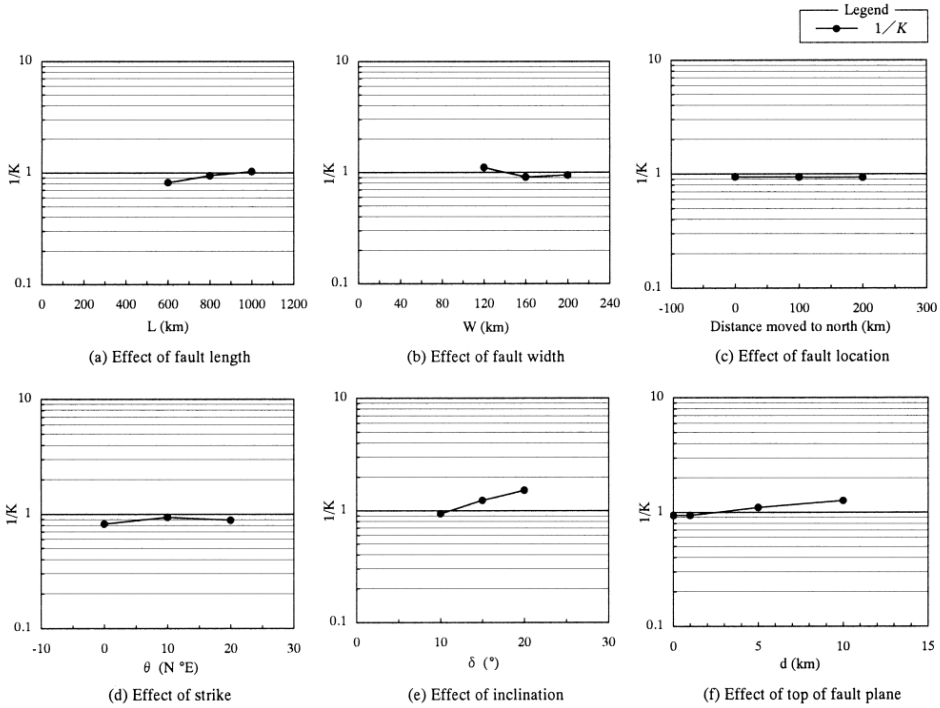

Figure 8: Relation of fault parameters and calculated tsunami heights.

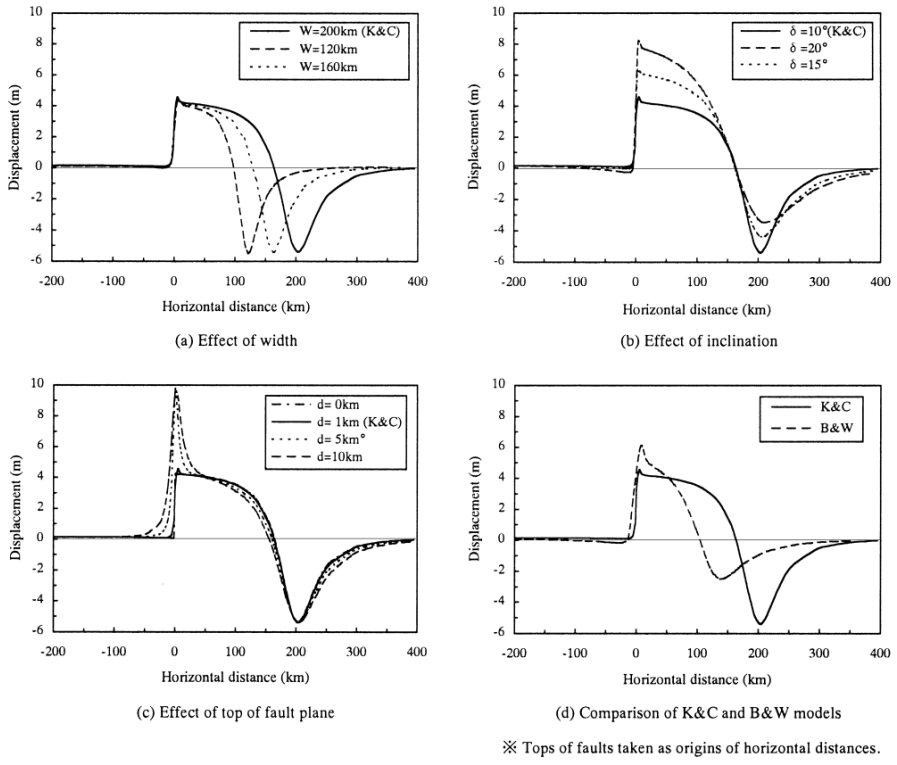

Figure 9: The sections of initial wave level distribution in principal cases.

Table 2: Fault parameters and calculated tsunami height indices.

		Length **L** (km)	Width **W** (km)	Slip **D** (m)	Strike $\boldsymbol{\theta}$ (N°E)	Inclination $\boldsymbol{\delta}$ (°)	Top depth of fault plane **d** (km)	Slip angle $\boldsymbol{\lambda}$ (°)	Earthquake moment $\mathbf{M_o}$ ($\times 10^{30}$ dyn cm)	Moment magnitude $\mathbf{M_w}$	Indices **K**	Indices $\boldsymbol{\kappa}$	Indices **1/K**
Kanamori and Cipar (1974) model		800	200	24	10	10	1	90	2.7	9.55	1.06	1.40	0.94
Length	L = 600 km	600	200	24	10	10	1	90	2.0	9.47	1.22	1.37	0.82
	L = 1000 km	1000	200	24	10	10	1	90	3.4	9.62	0.97	1.39	1.03
Width	W = 160 km	800	160	24	10	10	1	90	2.2	9.49	1.10	1.38	0.91
	W = 120 km	800	120	24	10	10	1	90	1.6	9.41	0.90	1.31	1.11
Location	100 km north	800	200	24	10	10	1	90	2.7	9.55	1.07	1.39	0.94
	200 km north	800	200	24	10	10	1	90	2.7	9.55	1.07	1.39	0.93
Strike	Strike + 10°	800	200	24	20	10	1	100	2.7	9.55	1.13	1.38	0.89
	Strike − 10°	800	200	24	0	10	1	90	2.7	9.55	1.22	1.34	0.82
Dip	$\delta = 15°$	800	200	24	10	15	1	80	2.7	9.55	0.81	1.38	1.24
	$\delta = 20°$	800	200	24	10	20	1	90	2.7	9.55	0.66	1.36	1.52
Depth of	d = 0 km	800	200	24	10	10	0	90	2.7	9.55	1.06	1.40	0.94
fault top	d = 5 km	800	200	24	10	10	5	90	2.7	9.55	0.90	1.36	1.11
	d = 10 km	800	200	24	10	10	10	90	2.7	9.55	0.79	1.34	1.27
Barrientos and Ward (1990) model		850	130	17	7	20	4	105	1.3	9.35	0.81	1.33	1.23

Observed inundation height confirmation site n = 117

For rigidity, $\mu = 7.0 \times 10^{11}$ dyn/cm^2 of K&C (1974) was used.

Equations:

$$\log K = \frac{1}{n}\sum_{i=1}^{n} \log K_i$$

$$\log \kappa = \left\{ \frac{1}{n}\sum_{i=1}^{n} (\log K_i)^2 - (\log K)^2 \right\}^{\frac{1}{2}}$$

n : number of sites

K_i : (observed inundation height)\(calculated value) of i-th site

From those figures, it is thought that the difference of inclination angle and the top depth of the fault plane give relatively large influence to the calculated tsunami wave height; however, as these parameters are mostly defined by the shape of the plate boundary, pre-understanding for the earthquake occurrence in the sea area could make the difference small. The differences due to length, width, location, and strike of the fault are within 20% in the average tsunami wave height; it is confirmed that the estimation error of parameter has little influence in calculated tsunami wave height.

4.3 Calculation time

This numerical simulation was performed using a personal computer (CPU: Pentium, 800 MHz). It took approximately 70 min for trans-Pacific propagation calculation, equal to the reproduction of 35 hours, and approximately 15 hours and 20 minutes for the Japanese coastal calculation, reproducing 12 hours including the run-up area of 93 × 93 m grids. As the maximum wave amplitude occurred at 8 hours after the tsunami wave arrived offshore of Japan, in the case of 8-hour reproduction, it is possible to shorten the calculating time to approximately 10 hours.

Therefore, it is possible that the calculation of trans-Pacific propagation and Japanese coastal finish sufficiently in a total of approximately 11 hours. As the propagation time of a tsunami from Chile is generally approximately 20 hours, it is assumed to be sufficiently possible to numerically forecast transoceanic tsunamis in real time.

5. Conclusions

1. Good reproducibility of tsunami heights and periodic characteristics distributed along the Japanese coast in the numerical simulation for the 1960 Chilean tsunami was obtained.

2. It was confirmed that the short-period components decayed by diffusion and the transoceanic tsunami waves consequently became long-period dominant, in addition to the tsunami source itself with long-period component.

3. It was found that estimation errors of fault parameters have little influence on tsunami wave heights calculated for the Japanese coast.

4. As the time required for calculations is approximately 11 hours, it is possible enough to carry out real-time numerical forecasts before transoceanic tsunami arrival.

To improve the accuracy of transoceanic tsunami forecasts, it is necessary to develop a method that can correct the calculation results using the tsunami wave height observed at the Hawaiian islands and/or by the tsunami gauges on the sea floor of the Pacific Ocean.

Acknowledgments. The authors gratefully acknowledge the valuable advice of

Professor Fumihiko Imamura of the Faculty of Engineering, Tohoku University in completing this paper.

6. References

Aida, I.(1978): Reliability of a tsunami source model derived from fault parameters. *J. Phys. Earth*, *26*, 57–73.

Barrientos, S.E., and S.N. Ward (1990): The 1960 Chile Earthquake: inversion for slip distribution from surface deformation. *Geophys. J. Int.*, *103*, 589–598.

Goto, C., and K. Sato (1993): Development of tsunami numerical simulation system for Sanriku coast in Japan. Report of the Port and Harbour Research Institute, 32(2), 4–44 (in Japanese).

Imamura, F., T. Nagai, H. Takenaka, and N. Shuto (1990): Computer graphics for the study of transoceanic propagation of tsunamis. *Proceedings of the 4th Pacific Congress of Marine Science and Technology (PACON) 90*, 118–123.

Iwasaki, T., and A. Mano (1979): Two-dimensional numerical simulation of tsunami run-ups in the Eulerian description. *Proceedings of the 26th Conference on Coastal Engineering*, JSCE, 70–74 (in Japanese).

Kanamori, H., and J.J. Cipar (1974): Focal process of the great Chilean earthquake May 22, 1960. *Phys. Earth Planet. Int.*, *9*, 128–136.

Mansinha, L., and D.E. Smylie (1971): The displacement fields of inclined faults. *Bull. Seismol. Soc. Am.*, *61*(5), 1433–1440.

Tanioka, Y. (2000): Numerical simulation of far-field tsunami using the linear Boussinesq equation—The 1998 Papua New Guinea tsunami. *Meteorol. Geophys.*, *51*(1), 17–25.

The Committee for Field Investigation of the Chilean Tsunami of 1960 (1961): Report on the Chilean tsunami of May 24, 1960, as observed along the coast of Japan. Maruzen, Tokyo, 397 pp. (in Japanese).

Tsuji, Y. (1991): Decay of the initial crest of the 1960 Chilean tsunami scattering of tsunami waves caused by sea mounts and the effects of dispersion. Proceedings of the 2nd UJNR Tsunami Workshop, 13–25.